HHS Public Access

Author manuscript

Sci Transl Med. Author manuscript; available in PMC 2015 July 23.

Published in final edited form as:

Sci Transl Med. 2014 July 23; 6(246): 246ra97. doi:10.1126/scitranslmed.3008889.

Some gating potentiators, including VX-770, diminish ΔF508-CFTR functional expression

Guido Veit[1], **Radu G. Avramescu**[1], **Doranda Perdomo**[1], **Puay-Wah Phuan**[2], **Miklos Bagdany**[1], **Pirjo M. Apaja**[1], **Florence Borot**[1], **Daniel Szollosi**[3,4], **Yu-Sheng Wu**[1], **Walter E. Finkbeiner**[5], **Tamas Hegedus**[3,4], **Alan S. Verkman**[2], and **Gergely L. Lukacs**[1,6,7,*]

[1]Department of Physiology, McGill University, Montréal, Quebec H3G 1Y6, Canada.

[2]Departments of Medicine and Physiology, University of California, San Francisco, San Francisco, CA 94143–0521, USA.

[3]MTA-SE Molecular Biophysics Research Group, Hungarian Academy of Sciences, 1444 Budapest, Hungary.

[4]Department of Biophysics and Radiation Biology, Semmelweis University, 1444 Budapest P.O. Box 263, Hungary.

[5]Department of Pathology, University of California, San Francisco, San Francisco, CA 94143–0511, USA.

[6]Department of Biochemistry, McGill University, Montréal, Quebec H3G 1Y6, Canada.

[7]Groupe de Recherche Axé sur la Structure des Protéines (GRASP), McGill University, Montréal, Quebec H3G 1Y6, Canada.

Abstract

Cystic fibrosis (CF) is caused by mutations in the CF transmembrane regulator (CFTR) that result in reduced anion conductance at the apical membrane of secretory epithelia. Treatment of CF patients carrying the G551D gating mutation with the potentiator VX-770 (ivacaftor) largely restores channel activity and has shown substantial clinical benefit. However, most CF patients carry the ΔF508 mutation, which impairs CFTR folding, processing, function, and stability. Studies in homozygous ΔF508 CF patients indicated little clinical benefit of monotherapy with the investigational corrector VX-809 (lumacaftor) or VX-770, whereas combination clinical trials

*Corresponding author. gergely.lukacs@mcgill.ca.

Author contributions: The overall design of the study was by G.V. and G.L.L.; G.V., R.G.A., D.P., P.-W.P., M.B., and P.M.A. performed experiments and analyzed the results. D.S. and T.H. performed the molecular dynamics simulations and in silico docking. W.E.F. contributed the primary HBE cells. F.B. and Y.-S.W. cloned the CFTR constructs. The manuscript was primarily written by G.V., G.L.L., and A.S.V. with input from all authors.

Competing interests: GLL has consulted for Genzyme in 2011–2012 and has also served as an unpaid advisor to CFFT Inc. All other authors declare that they have no competing interests.

Data and materials availability: CFBE41o− cell lines were obtained under material transfer agreement (MTA) from D. Gruenert (UCSF). CFTR expression constructs are available under MTA from McGill University.

SUPPLEMENTARY MATERIALS

www.sciencetranslationalmedicine.org/cgi/content/full/6/246/246ra97/DC1

Materials and Methods

References (67–70)

show limited but significant improvements in lung function. We show that VX-770, as well as most other potentiators, reduces the correction efficacy of VX-809 and another investigational corrector, VX-661. To mimic the administration of VX-770 alone or in combination with VX-809, we examined its long-term effect in immortalized and primary human respiratory epithelia. VX-770 diminished the folding efficiency and the metabolic stability of ΔF508-CFTR at the endoplasmic reticulum (ER) and post-ER compartments, respectively, causing reduced cell surface ΔF508-CFTR density and function. VX-770–induced destabilization of ΔF508-CFTR was influenced by second-site suppressor mutations of the folding defect and was prevented by stabilization of the nucleotide-binding domain 1 (NBD1)–NBD2 interface. The reduced correction efficiency of ΔF508-CFTR, as well as of two other processing mutations in the presence of VX-770, suggests the need for further optimization of potentiators to maximize the clinical benefit of corrector-potentiator combination therapy in CF.

INTRODUCTION

Cystic fibrosis (CF), one of the most common inherited diseases in the Caucasian population, is caused by mutations in the CF transmembrane regulator (*CFTR*) gene that lead to loss of CFTR channel function and impaired epithelial anion transport in the lung, intestine, pancreas, and other organs (1, 2). The nearly 2000 different mutations identified in the *CFTR* gene (http://www.genet.sickkids.on.ca) have been categorized into six different classes according to the resulting molecular aberration (3, 4). The most prevalent class II mutation, deletion of phenylalanine 508 (ΔF508), results in misfolded CFTR channels that are predominantly recognized and degraded by the endoplasmic reticulum (ER) quality control machinery (2, 5). ΔF508-CFTR molecules that escape from the ER are functionally impaired (class III mutation) and conformationally unstable, with rapid removal from the plasma membrane (PM) by the peripheral quality control and targeting for endolysosomal degradation (6). G551D, the third most common CF-causing mutation that affects ~4% of CF patients, belongs to class III and displays normal processing and cell surface expression but severe functional impairment (7).

The CFTR protein is an ATP (adenosine 5′-triphosphate)–binding cassette transporter family member that comprises two membrane-spanning domains (MSD1 and MSD2) and three cytosolic domains, two nucleotide-binding domains (NBD1 and NBD2) and a regulatory domain (8). The ΔF508 mutation in the NBD1 produces multiple structural defects in CFTR. At least two of those, NBD1 misfolding and NBD1-MSD1/2 interfacial instability, have to be reversed genetically and/or pharmacologically to achieve near wild type–like PM expression (9–13).

Mechanistically, the available investigational small-molecule CFTR modulators fall into three classes: (i) suppressor molecules that prevent premature termination of protein synthesis; (ii) correctors that partially revert the folding and processing defects; and (iii) potentiators that increase channel gating and conductance (14–16). The potentiator ivacaftor (VX-770, Kalydeco) has been approved for therapy of CF patients with one copy of G551D (17) or some other rare gating mutations (18, 19). VX-770 treatment of patients with G551D and other class III mutations demonstrated marked clinical benefit, including ~10 to 14%

increase in the forced expiratory volume in 1 s (FEV_1), decrease in pulmonary exacerbations, and weight gain relative to placebo treatment (20–22).

Nasal potential difference and short-circuit current (I_{sc}) measurements in rectal biopsies of CF patients as well as in primary human bronchial epithelial (HBE) cells indicate that a subset of homozygous ΔF508 patients have residual ΔF508-CFTR PM function (23–25). The PM expression and activity of ΔF508-CFTR inversely correlate with CF disease severity (23, 25, 26). Acute addition of VX-770 in HBE cell cultures from some patients homozygous for the ΔF508 mutation increased the residual forskolin-stimulated channel activity from ~4 to 16% of that in HBE cultures from non-CF individuals, whereas other cultures were not responsive (24). A phase 2 trial in ΔF508 homozygous patients, however, showed no improvement in FEV_1, although a small reduction in sweat chloride concentration upon VX-770 treatment occurred (27).

Likewise, treatment with VX-809 (lumacaftor) alone, a promising investigational corrector drug that restores the ΔF508-CFTR PM expression and function to ~15% of wild-type CFTR activity in non-CF HBE cells (28), failed to show robust improvement in lung function of Δ*F508*/Δ*F508* patients (29). In cell cultures, a combination of chronic VX-809 and acute VX-770, together with a cAMP (cyclic adenosine 3′,5′-monophosphate) agonist, increased ΔF508-CFTR conductance to ~25% of that in non-CF HBE (28). These preclinical results motivated the ongoing phase 2–3 clinical trials of combination treatment with VX-770 and VX-809, or VX-661, another investigational corrector (14) (http://www.clinicaltrials.gov NCT01225211 and NCT01531673). The results of a phase 2 trial in homozygous ΔF508 patients receiving VX-809 and VX-770 combination treatment suggested an improvement in FEV_1 of 8.6% compared to placebo ($P < 0.001$) and amarginal decrease in sweat chloride concentration (30), although sustained clinical benefit awaits verification. The recent news release of the first phase 3 trials reported a mean absolute improvement in FEV_1 compared to placebo in the range of 2.6 to 4.0% ($P \leq 0.0004$) (31). The limited clinical efficacy of combination therapy based on these data may be accounted for by insufficient tissue concentration of the drugs, decreased susceptibility to correction in the inflamed lung, and/or conformational destabilization of the mutant upon chronic exposure to VX-770. To evaluate the latter possibility, we determined the effect of prolonged exposure to VX-770, and to other investigational potentiators, on the biochemical and functional expression of ΔF508-CFTR. The results indicate that VX-770 and some, but not all, other potentiators cause ΔF508-CFTR destabilization at multiple cellular sites in model systems and primary CF HBE, with consequent reduced functional expression of ΔF508-CFTR at the cell surface.

RESULTS

Prolonged exposure to VX-770 reduces the PM and cellular expression of ΔF508-CFTR

To investigate the effect of prolonged exposure to VX-770 on ΔF508-CFTR PM expression, we first used the human CF bronchial epithelial cell line CFBE41o− (referred to as CFBE), a widely validated model system with $CFTR^{\Delta F508/\Delta F508}$ genetic background but no detectable CFTR protein expression (32). CFBE cells were engineered for inducible expression of CFTR variants as described (10, 33). To facilitate the PM detection of ΔF508-CFTR,

horseradish peroxidase isoenzyme C (HRP-C) was genetically engineered into its fourth extracellular loop. The functional and biochemical properties of ΔF508-CFTR-HRP are similar to those of the 3HA-tagged variant (13, 34) (fig. S1, A to D).

Acute addition of VX-770 to low temperature–rescued ΔF508-CFTR (rΔF508) in CFBE cells increased the cAMP-dependent protein kinase (PKA)–activated current by up to sixfold with EC_{50} of 12.8 ± 1.0 nM (fig. S2, A and B), similar to that reported in ΔF508/ΔF508 HBE cells (22 ± 10 nM) (24). Prolonged exposure (24 hours) to VX-770, however, caused a concentration-dependent decrease in the PM density of ΔF508-CFTR, regardless of whether the preincubation with VX-770 was done at physiological temperature or at 26 to 30°C, which facilitated ΔF508 CFTR biosynthetic processing (Fig. 1, A and B). The maximal reduction in ΔF508-CFTR PM density was attained at ~30 nM VX-770, well below the plasma concentration of ~3.5 μM in VX-770–treated CF patients (35). Although increasing the concentration of human serum (0 to 100%) raised the EC_{50} of VX-770 from 2.5 ± 0.2 nM to 23.1 ± 4.6 nM in the presence of VX-809, it did not affect the reduced PM density achieved by long-term treatment with ≥100 nM VX-770 (fig. S2, G and H). In contrast, the PM density of wild-type CFTR or G551D-CFTR was not reduced by prolonged VX-770 exposure (Fig. 1, A and C).

VX-809 partially restored ΔF508-CFTR biogenesis, function, and PM expression by about three- to fourfold in CFBE and primary HBE monolayers (fig. S2C) (10, 13, 28). VX-809 alone or in combination with low-temperature rescue, however, failed to prevent the VX-770–dependent reduction in ΔF508-CFTR PM density (Fig. 1, A and B, and fig. S2C). Similar results were obtained for ΔF508-CFTR rescued with the corrector VX-661 (fig. S2D). The VX-770–induced reduction in ΔF508-CFTR PM density was independent of channel gating because neither activation of adenyl cyclase by forskolin nor blocking the channel with BPO-27 (36) influenced the VX-770 effect (Fig. 1B and fig. S2C). Extended exposure to VX-770 did not affect cell viability (fig. S2E). PM down-regulation of 3HA-tagged ΔF508-CFTR by VX-770 in low temperature–rescued CFBE, NCI-H441 (a lung adenocarcinoma cell line exhibiting some Clara cell features), and MDCK II (Madin-Darby canine kidney) epithelial cells suggested that the VX-770 effect is not CFBE-specific or related to the HRP-tag insertion (Fig. 1D and fig. S2F).

To evaluate whether VX-770 causes the redistribution of PM resident ΔF508-CFTR to intracellular pools or exerts a global down-regulation of mature ΔF508-CFTR in post-ER compartments, we determined the cellular expression of ΔF508-CFTR by immunoblot analysis. VX-770 treatment for 24 hours decreased the amount of the complex-glycosylated ΔF508-CFTR (C-band) in CFBE lysates in a dose-dependent manner (Fig. 1E). The VX-770 effect was attenuated in VX-809– or VX-661–treated cells, probably due to partial stabilization of the mature ΔF508-CFTR pool by VX-809, as reported previously (Fig. 1, F and G) (10, 28, 37). In contrast, the complex-glycosylated form of wild-type CFTR and G551D-CFTR was not affected by prolonged VX-770 exposure (Fig. 1H). The modest, albeit significant ($P = 0.02$), decrease in the steady-state level of core-glycosylated ΔF508-CFTR (B-band) may be due to reduced biogenesis and/or accelerated ER degradation upon exposure to 100 nM VX-770 (Fig. 1, E to G). These observations suggest that the VX-770

effect cannot be explained merely by accelerated internalization or impeded recycling of rΔF508-CFTR.

ΔF508-CFTR chloride conductance decreases after long-term VX-770 exposure in CFBE and primary respiratory epithelia

To assess the functional consequence of prolonged VX-770 exposure of CFBE and primary HBE cells, we performed short-circuit current (I_{sc}) measurements after 24 hours of incubation with 100 nM VX-770. Forskolin-stimulated I_{sc} was measured after inhibition of ENaC (epithelial sodium channel) by amiloride and maximal acute potentiation of cell surface ΔF508-CFTR function with 10 μM VX-770 (Fig. 2A). Forskolin-stimulated I_{sc} (1.7 ± 0.3 μA/cm^2) was reduced to 1.1 ± 0.2 μA/cm after incubation of ΔF508-CFTR–expressing CFBE cells with VX-770 for 24 hours. A comparable reduction in I_{sc} was observed in VX-809– and VX-661–corrected cells (Fig. 2, A and B).

To confirm the relevance of these results to human tissues, we assessed the VX-770 effect in primary HBE cell cultures, isolated from the lungs of six $CFTR^{\Delta F508/\Delta F508}$ patients and four $CFTR^{WT/WT}$ donors. The HBE cells were differentiated on Snapwell filter inserts under air-liquid interface (ALI) conditions for at least 4 weeks either in Ultroser G medium (i), which increases the ENaC- and CFTR-mediated currents (38), or in ALI medium (ii) (39) (Fig. 2, C and D). The residual CFTR-mediated I_{sc} in the ΔF508-CFTR HBE was augmented by treatment with the correctors VX-809 or VX-661 (3 μM, 24 hours) (13). To further increase CFTR-mediated I_{sc} and isolate the apical anion conductance, some cells were differentiated in Ultroser G medium and analyzed after basolateral permeabilization and in the presence of a basolateral-to-apical Cl^- gradient. Independent of the differentiation method and presence of a chloride gradient, exposure to VX-770 for 24 hours decreased the VX-809– or VX-661–corrected ΔF508-CFTR current by 33 ± 6% and 47 ± 8% (mean ± SEM, $n = 6$), respectively (Fig. 2, C and D, and Table 1). In contrast, VX-770 pretreatment did not affect the PKA-activated wild-type CFTR current in HBE (Fig. 2E and table S1), in line with the absence of changes in PM and C-band density in wild-type CFTR (Fig. 1H).

Potentiator P5 does not impair the PM density and function of ΔF508-CFTR

To determine whether down-regulation of rΔF508-CFTR is a universal phenomenon of long-term potentiator exposure, we tested a panel of CFTR potentiators with distinct chemical structures. These investigational small molecules, abbreviated as P1 to P10, were made available by the Cystic Fibrosis Foundation Therapeutics Inc. (CFFT) for the research community (fig. S3A). The potency and efficacy of P1 to P10 on the activity of low-temperature rΔF508-CFTR were demonstrated in CFBE cells using the halide-sensitive yellow fluorescent protein (YFP) quenching assay. Acute addition of P1 to P8 confirmed the potentiation of the rΔF508-CFTR activity, whereas P9 and P10 had only small effects (Fig. 3, A to H, and fig. S3, B to D). The dose-response curve of genistein (P6), a flavone widely used for acute potentiation of CFTR activity, did not reach saturation activity at 100 μM, suggesting that rΔF508-CFTR has lower affinity for genistein than wild-type CFTR (40, 41) (Fig. 3F).

Prolonged treatment (24 hours) with most potentiators produced a concentration-dependent decrease in ΔF508-CFTR PM density in CFBE partially rescued with low temperature alone or in combination with VX-809 (Fig. 3, A to H). This was especially prominent for genistein (P6), with ~60 and ~75% decrease in rΔF508-CFTR PM density and conductance, respectively (Fig. 3, F, I, and J). P5 did not reduce the ΔF508-CFTR PM density and potentiated the rΔF508-CFTR activity by up to about sevenfold in CFBE cells (Fig. 3E). This result was confirmed by immunoblot analysis of low-temperature and VX-809 rΔF508-CFTR. Increasing concentrations of P5 did not alter the relative abundance of core- and complex-glycosylated ΔF508-CFTR, suggesting that P5 does not affect ΔF508-CFTR ER processing and stability (Fig. 4A).

I_{sc} measurements in CFBE expressing ΔF508-CFTR and primary HBE cells isolated from four *CFTR*$^{\Delta F508/\Delta F508}$ patients also confirmed the lack of effect of prolonged P5 exposure on the maximal activation of ΔF508-CFTR current at physiological temperature (Fig. 4, B and C, and Table 1). P5 may thus be a useful investigational compound to potentiate ΔF508-CFTR function without impairing its PM expression.

VX-770 impairs biogenesis, stability, and endocytic trafficking of the ΔF508-CFTR

Because VX-770 may impair both the biogenesis and the metabolic stability of mature ΔF508-CFTR, according to the immunoblot analysis, we measured conformational maturation of newly formed ΔF508 CFTR by the metabolic pulse-chase technique (11). Phosphorimage analysis was used to quantify the conversion efficiency of core-glycosylated ΔF508-CFTR (B-band), labeled with [^{35}S]methionine and [^{35}S]cysteine, into complex-glycosylated ΔF508-CFTR (C-band) upon traversing the cis/medial Golgi in CFBE cells. The folding efficiency of ΔF508-CFTR in the presence of VX-809 decreased from 1.8 ± 0.2% to 1.3 ± 0.1% after VX-770 treatment for 24 hours, representing a ~25% (P = 0.026) reduction (Fig. 5A, left panel). Similarly, the folding efficiency of VX-770–treated ΔF508-CFTR-3S, carrying NBD1-stabilizing second-site mutations, decreased from 4.0 ± 0.2% to 2.6 ± 0.6% (P = 0.049) (Fig. 5A, right panel). The reduced ER maturation efficiency cannot be attributed to decreased transcription or profoundly increased degradation of the core-glycosylated ΔF508-CFTR because neither the mRNA level nor the B-band stability was affected by VX-770 (fig. S4, A to C). The decreased incorporation of radioactivity during the 30-min pulse is consistent with increased cotranslational degradation and/or partial translational inhibition (fig. S4D).

The peripheral stability of rΔF508-CFTR was determined both at the PM and in post-ER compartments in CFBE cells. After the accumulation of low temperature–rescued ΔF508-CFTR at the PM, it was rapidly removed with a $T_{1/2}$ ~2.5 hours at 37°C (Fig. 5B), probably as a result of accelerated internalization, lysosomal targeting, and attenuated recycling, as reported in HeLa cells (6). The $T_{1/2}$ of rΔF508-CFTR at the PM was decreased by VX-770 to ~1.75 hours, regardless of whether VX-770 was present for 24 or 3 hours (Fig. 5B). VX-770 also accelerated the PM turnover of rΔF508-CFTR that was modestly stabilized by VX-809 (28), as reflected by the reduction of $T_{1/2}$ from ~3 to ~2.25 hours (Fig. 5C). In addition, VX-770 destabilized the complex-glycosylated rΔF508-CFTR pool both in the presence and in the absence of VX-809, as determined by cycloheximide (CHX) chase and

immunoblot (Fig. 5, D and E). Similar results were obtained by metabolic pulse-chase for rΔF508-CFTR containing the 3S NBD1 stabilizing mutation (fig. S4E). Together, these observations suggest that VX-770 interferes with both the biogenesis and the peripheral stability of mature ΔF508-CFTR in the presence or absence of VX-809, which likely accounts for reduced ΔF508-CFTR PM function. As found for VX-770, prolonged treatment with potentiators P1, P2, P4, P6, and P7 led to a destabilization of PM-localized rΔF508-CFTR (Fig. 5F). Notably, destabilization was not seen in CFBE treated with P3 or P5 (Fig. 5F).

The conformational destabilization of rΔF508-CFTR by VX-770 may be recognized by the peripheral quality control machinery that targets non-native PM proteins for lysosomal degradation (42). This possibility was assessed by determining the post-endocytic fate of rΔF508-CFTR by measuring the pH of CFTR-containing endocytic vesicles with fluorescence ratio image analysis (FRIA) (43). rΔF508-CFTR was accumulated in polarized, filter-grown CFBE at reduced temperature and exposed for 24 hours to DMSO,VX-809,VX-770, or VX-809 + VX-770. The rΔF508-CFTR-3HA was unfolded at 37°C for 1.5 hours and then labeled with pH-sensitive FITC (fluorescein isothiocyanate) at 0°C, using the antibody capture technique as described in Materials and Methods. Internalization of labeled PM ΔF508-CFTR was initiated by shifting the temperature to 37°C.

Endocytosed rΔF508-CFTR was delivered after 30 min into multivesicular bodies (MVB)/lysosomes (pH 5.25 ± 0.01), whereas wild-type CFTR largely remained in early endosomes (Fig. 5, G and H, and fig. S4F). MVB/lysosomal delivery was inhibited by VX-809, as seen by preferential confinement to early endosomes (pH 6.31 ± 0.1) during a 2-hour chase (Fig. 5, G and H). VX-770 partially reversed the VX-809 trafficking effect by facilitating rΔF508-CFTR transfer to late endosomes, as indicated by the pH (5.84 ± 0.1) of the rΔF508-CFTR–containing vesicular compartment after a 2-hour chase (Fig. 5, G and H), suggesting that VX-770 increases ΔF508-CFTR susceptibility to recognition by the peripheral quality control machinery.

The effect of VX-770 at the single-molecule level was measured by determining the channel function of rΔF508-CFTR with or without second-site suppressor mutations in reconstituted planar phospholipid bilayer (Fig. 6, A to E). R29K and R555K mutations were introduced (ΔF508-CFTR-2RK) to increase channel reconstitution efficiency (44). The open probability (P_o) of phosphorylated ΔF508-CFTR-2RK channel decreased from 0.19 to 0.09 upon increasing the temperature from 24 to 36°C (Fig. 6B). VX-770 enhanced ΔF508-CFTR-2RK function at low temperature (P_o = 0.43 at 24°C), but accelerated its inactivation rate, as indicated by the ~3.5-fold faster loss of channel activity between 32 and 36°C (−18.1 ± 1.4%/°C in the presence of VX-770 versus −4.9 ± 2.8%/°C inactivation rate in the control) (Fig. 6, A to C). These results suggest a direct interaction of VX-770 with ΔF508-CFTR-2RK, resulting in its destabilization.

Second-site mutations modulate ΔF508-CFTR susceptibility to VX-770–mediated down-regulation

Second-site suppressor mutations in ΔF508-CFTR have been used to investigate mechanisms of small-molecule CFTR modulators (10) (fig. S5A). An increasing number of solubilizing mutations (1S, 2S, and 3S) progressively stabilize the isolated ΔF508-NBD1 domain energetically (see table S2 for list of all mutants) (11, 45–47). Similarly, NBD1-MSD2 interface–stabilizing mutants (for example, R1070W or V510D) (8, 48) enhance the PM expression of ΔF508-CFTR PM to ~5 to 10% of wild-type CFTR. Combining the two classes of mutations increased expression to ~50% of wild-type CFTR by aiding coupled domain folding (10, 11). Unexpectedly, neither solubilizing nor interface-stabilizing mutations alone or in combination prevented the reduction in ΔF508-CFTR expression after prolonged VX-770 exposure, regardless of the presence of VX-809 (Fig. 7, A and B, and fig. S5, B to F). Solubilizing mutations augmented the loss of ΔF508-CFTR PM expression by VX-770 from ~45 to ~80% and decreased the IC_{50} of VX-770 from ~10 nM to 1 to 2 nM (P = 0.0020 to 0.0153) (Fig. 7, A to C, and fig. S5, B and C). In contrast, the C-terminal 70–amino acid truncation (Δ70 CFTR), which reduced the PM stability and expression by ~90% relative to wild-type CFTR (49), was resistant to prolonged VX-770 treatment (Fig. 7A and fig. S5G). The lack of apparent correlation between global down-regulation of ΔF508-CFTR PM density and the extent of VX-770–induced destabilization is further supported by the phenotype of revertant mutations [3R; G550E, R553Q, and R555K (50)] alone or in combination with 1S (R1S). These mutations energetically stabilize the ΔF508-NBD1 to an extent comparable to 3S, increase the PM density to ~40 to 50% of wild-type CFTR (11), and either directly or indirectly delay NBD1-NBD2 dimer dissociation (11, 51) and channel closing, manifesting in about twofold increased P_o (Fig. 6D and fig. S6A). 3R or R1S mutations prevented the VX-770–induced down-regulation of ΔF508-CFTR from the PM (Fig. 7, A and D, and fig. S5H), and the R1S mutation eliminated the thermal inactivation in the bilayer and attenuated the potentiating effect of VX-770 (Fig. 6D and fig. S6A). Similarly, the ΔF508-E1371S (E1371S) mutation, which increases NBD1-NBD2 dimer stability by preventing the hydrolysis of bound ATP to the Walker A and B motifs in NBD2 and thereby the dissociation of the NBD1-NBD2 dimer (52, 53), protected ΔF508-CFTR from thermal inactivation in reconstituted planar phospholipid bilayer experiments regardless of the presence of VX-770 (Fig. 6E and fig. S6B).

To offer a possible explanation for the VX-770 interaction with ΔF508-CFTR, we propose the formation of multiple binding pockets in the partially unfolded ΔF508-NBD1/2, based on molecular dynamics simulations and docking studies (fig. S7A). The putative binding sites of VX-770 are labeled in red in the ΔF508-CFTR structure (fig. S7B). High-affinity/low binding energy (less than −6.5 kcal/mol) interactions of VX-770 with amino acids in the NBD1/2 interface and the coupling helix of CL1 in ΔF508-CFTR only partially overlap with those in wild-type CFTR (fig. S7C), consistent with the absence of the destabilizing effect of VX-770 in wild-type CFTR. The lack of VX-770 destabilizing effect on the revertant and NBD2 ATPase (adenosine triphosphatase) mutants is in line with the notion that prolonged NBD1-NBD2 dimerization (51, 54) either directly or allosterically hinders the VX-770 association with destabilizing sites. Although the dockings studies

suggest partially overlapping putative binding sites for P5 and VX-770, P5 also has unique interactions in NBD1 (amino acids 621 to 623) that are not observed for VX-770 (fig. S7D).

Rare CF mutations sensitize CFTR to VX-770–induced down-regulation

Gating potentiation of class III mutations by acute VX-770 exposure in preclinical settings rationalized the approval of ivacaftor in patients with eight rare CF mutations (19). To evaluate whether prolonged VX-770 exposure may interfere with the expression of other class III and class II mutations, we determined the PM density and function of R347H-, R170G-, and P67L-CFTR (fig. S8A) in CFBE. Whereas R347H-CFTR, a class III mutation (55), was resistant to VX-770, PM expression was reduced by 30 to 43% and forskolin-stimulated I_{sc} was reduced by 32 to 38% in VX-809–rescued R170G-CFTR and P67L-CFTR by VX-770 (Fig. 7, E to H, and fig. S8, B and C), raising the possibility that multiple class II mutations are susceptible to VX-770–mediated destabilization.

DISCUSSION

Here, we provide evidence that basal and VX-809– or VX-661–rescued PM densities of ΔF508-CFTR are reduced in parallel with the loss of chloride conductance upon prolonged exposure to VX-770. The reduction in channel density was not prevented by partial correction of the ΔF508-CFTR biogenesis defect by low temperature. In contrast, the PM expression of wild-type CFTR and G551D-CFTR was not reduced by prolonged VX-770 treatment.

Although the cellular basis of the destabilizing action of VX-770 on ΔF508-CFTR is well documented both in this work and in an accompanying publication (56), its molecular details remain to be elucidated. Although indirect effect cannot be ruled out, we postulate that direct association of VX-770 with ΔF508-CFTR increases its unfolding propensity, an inference supported by the accelerated rate of functional inactivation of temperature-rescued ΔF508-CFTR-2RK in reconstituted planar lipid bilayers. The conformational destabilization of ΔF508-CFTR by VX-770 is also in line with its reduced ER folding efficiency, accelerated PM, and post-ER pool turnover, as well as lysosomal targeting from early endosomes, phenomena that have been described as hallmarks of the peripheral quality control of non-native membrane proteins (6, 42).

Conformational stabilization of NBD1 or the NBD1-MSD2 interface with second-site mutations (1S, 2S, or 3S and R1070W or V510D, respectively) sensitized ΔF508-CFTR to VX-770, as reflected by the increased fractional down-regulation and decreased IC_{50} (from ~10 to ~2 nM) despite partial rescue of misprocessing of these mutant variants (11). Despite conferring similar energetic stabilization as NBD1-3S, the revertant mutations that are clustered at residues 550 to 555 (11) bestowed complete resistance to PM down-regulation and thermal functional inactivation in the bilayer by VX-770. Because the revertant mutations probably stabilize the NBD1-NBD2 dimer (51), this observation suggests that an unstable NBD1-NBD2 interface is a prerequisite for the VX-770 destabilizing action, an inference that is supported by the resistance of ΔF508-CFTR-E1371S to VX-770. The E1371S substitution retards channel closing by preventing the hydrolysis of bound ATP to

the Walker A and B motifs in NBD2 and thereby the dissociation of the NBD1-NBD2 dimer (52, 53).

Monotherapy with VX-809, which increased ΔF508-CFTR–mediated I_{sc} to ~14% of that in wild-type CFTR in primary HBE (28), did not confer substantial clinical benefit (29). The maximally stimulated I_{sc} in VX-809–rescued ΔF508/ΔF508-HBE in combination with acute VX-770 potentiation reached ~23% of that in non-CF HBE in our studies (Table 1 and table S1). These results are consistent with published data suggesting an I_{sc} equivalent to ~25% of that in non-CFHBE (twofold increase over VX-809 alone) (28). Prolonged VX-770 exposure reduced the ΔF508 I_{sc} by 33 ± 6% (mean ± SEM, n = 6) in VX-809–corrected HBE, albeit with a considerable range of values in cells from different CF patients (12 to 49%, Table 1), which is likely due to the influence of the genetic or epigenetic variability between individuals on the proteostasis network activity (57, 58). In VX-661–rescued ΔF508/ΔF508-HBE, the VX-770–induced functional attenuation ranged between 14 and 65% with a mean of 47 ± 8% (± SEM, n = 6) (Table 1). If these results translate to the clinical setting, combination of corrector therapy with VX-770 could be beneficial for a subpopulation of ΔF508 CF patients, but may reduce the overall rescue efficiency below the threshold required for clinical benefit in poor VX-809 responders and/or individuals susceptible to VX-770–mediated channel destabilization. The negative action of VX-770 would be more pronounced in patients having a single copy of ΔF508-CFTR.

A limitation of our study is that the concentration of free VX-770 in lung cells of CF patients treated with VX-770 is not known, and hence, the VX-770–induced down-regulation of ΔF508-CFTR can only be extrapolated. VX-770 treatment with the recommended dose of 150 mg every 12 hours produced a peak plasma concentration of 3.5 μM after 5 days (35). Because ~97% of VX-770 is bound to plasma protein (35, 59), the free drug concentration is estimated to be ~100 nM in vivo, which is in line with its clinical benefit in patients carrying at least one G551D allele (21, 22) despite its relatively high EC_{50} for activation of G551D-CFTR (236 nM VX-770) in primary HBE (24). In our studies, maximal reduction of ΔF508-CFTR PM density and function was seen at ~30 nM VX-770 in CFBE. The effective in vivo intracellular concentration of VX-770, however, could be even higher than predicted due to the accumulation of VX-770 in primary HBE cells (56) and its eightfold enrichment in the epithelial lining fluid of the rat lung relative to plasma (59).

Because CFTR-mediated transepithelial transport is closely correlated with CF disease severity (23, 25, 60), evaluation of sustained exposure to modulators should be valuable in identifying individuals who would benefit from corrector-potentiator combination therapy with, for example, patient-derived primary or conditionally reprogrammed respiratory cells (61), or intestinal organoids (62). As a complementary strategy, new potentiators might be identified that lack the ΔF508-CFTR destabilizing action, as exemplified by the P5 (63). P5 efficiently stimulated the activity of phosphorylated rΔF508-CFTR, but not G551D (63). The latter suggests that the mechanism of action of P5 is distinct from that of VX-770 and therefore could be valuable to correct the gating defect of ΔF508-CFTR while preserving its PM density.

In summary, our results suggest that VX-770, as well as most of the available investigational potentiators, impairs the biochemical stability of ΔF508-CFTR and other class II processing mutations (such as P67L and R170G). These findings in cell cultures may translate to reduced efficacy of corrector-potentiator combination therapy in the clinical setting. Further structure-activity studies of existing potentiators, as well as identification of potentiators that do not destabilize mutant CFTRs, are warranted to enhance the therapeutic benefit of corrector-potentiator combination therapy in CF.

MATERIALS AND METHODS

Study design

The goal of the study was to measure the effect of long-term administration of VX-770 and other investigational potentiators, either alone or in combination with small-molecule correctors, on the biochemical and functional expression of ΔF508-CFTR in immortalized and primary human respiratory epithelia. CFBE heterologously expressing wild-type, G551D-, or ΔF508-CFTR and primary HBE with a $CFTR^{WT/WT}$ (from four donors) or a $CFTR^{\Delta F508/\Delta F508}$ (from six patients) genotype were subjected to chronic treatment with VX-770 (24 hours) in the presence or absence of the correctors VX-809 or VX-661, and CFTR function was determined by short-circuit current measurement or halide-sensitive YFP fluorescence quenching. The PM density, PM stability, cellular expression, conformational maturation, metabolic stability, and lysosomal targeting of ΔF508-CFTR were determined in CFBE to examine the cellular phenotype of the VX-770 destabilizing action. To elucidate the molecular mechanism of the VX-770 effect, we examined the functional destabilization of the mutant in a planar lipid bilayer and investigated the PM density and function of ΔF508-CFTR containing second-site mutations. Putative binding sites of potentiators were identified by molecular dynamic simulation and in silico docking. Finally, to assess the VX-770 effect specificity, the PM density and function of other class III and class II mutations (R347H-, R170G-, and P67L-CFTR) were determined in CFBE.

Antibodies and reagents

Mouse monoclonal anti–hemagglutinin (HA) anitbody was purchased from Covance Innovative Antibodies. VX-770, VX-809, and VX-661 were acquired from Selleckchem. The CFTR potentiators P1 to P10 were made available by R. J. Bridges (Rosalind Franklin University of Medicine and Science) and CFFT. All other chemicals were purchased from Sigma-Aldrich at the highest grade available.

Cell lines

Full-length human CFTR variants with the 3HA-tag in the fourth extracellular loop have been described before (10). The HRP-C was introduced into the fourth extracellular loop replacing the 3HA-tag by using the Eco RV/Avr II restriction sites with a 5′ linker (ctcgaatcaggaggtagtggtggcggaagt). The CFTR variants used in this study are listed in table S2. Maintenance of the human CF bronchial epithelial cell line CFBE41o− (32), with a $CFTR^{\Delta F508/\Delta F508}$ genotype [a gift from D. Gruenert, University of California, San Francisco (UCSF)], and stable cell line generation of CFTR-3HA variants under the control of a

tetracycline-responsive transactivator were described before (33). NCI-H441 and MDCK II cells expressing inducible ΔF508-CFTR have been described (10).

Primary HBE and short-circuit current measurements

Primary cultures of HBE cells from four *CFTR*$^{\Delta F508/\Delta F508}$ CF patients and four *CFTR*$^{WT/WT}$ donors were isolated and grown at ALI in ALI differentiation medium, as described (39, 64). Primary cultures differentiated in Ultorser G medium (38) from two *CFTR*$^{\Delta F508/\Delta F508}$ CF patients were purchased from ChanTest. I_{sc} measurements of primary HBE and CFBE epithelia were performed as described (33, 65).

PM density measurement

The PM density of 3HA-tagged CFTR variants was determined by cell surface enzyme-linked immunosorbent assay (ELISA) (6). HRP-tagged CFTR PM density was measured in a VICTOR Light Plate Reader (PerkinElmer) after addition of HRP-substrate (50 μl per well; SuperSignal West Pico, Thermo Fisher Scientific). PM density measurements were normalized with cell viability determined by alamarBlue Assay (Invitrogen).

Halide-sensitive YFP quenching assay

Assay of ΔF508-CFTR function by halide-sensitive YFP fluorescence quenching was performed as described (33). CFBE cells expressing inducible ΔF508-CFTR were transduced with lentiviral particles encoding the halide sensor YFP-F46L/H148Q/I152L (66) followed by isolation of double-expressing clones. YFP-expressing cells or controls were seeded onto 96-well microplates at a density of 2×10^4 cells per well, induced for ΔF508-CFTR expression for 2 days at 37°C, and low temperature–rescued for an additional 48 hours at 26°C. During the assay, cells were incubated in phosphate-buffered saline (PBS)–chloride (50 μl per well) (140 mM NaCl, 2.7 mM KCl, 8.1 mM Na_2HPO_4, 1.5 mM KH2PO_4, 1.1 mM $MgCl_2$, 0.7 mM $CaCl_2$, and 5 mM glucose, pH 7.4) containing the indicated potentiator concentrations, followed by well-wise injection of activator solution (50 μl per well) [20 μM forskolin, 0.5 mM 3-isobutyl-1-methyl-xanthine (IBMX), 0.5 mM 8-(4-chlorophenylthio)-adenosine-3′,5′-cyclic monophosphate (cpt-cAMP)] and 100 μl of PBS-iodide, in which NaCl was replaced with NaI. The fluorescence was monitored for 36 s with a 5-Hz acquisition rate at 485-nm excitation and 520-nm emission wavelengths using a POLARstar OPTIMA (BMG LABTECH) fluorescence plate reader. After background subtraction and normalization to YFP signals before NaI injection, the I^- influx rate was calculated by linear fitting to the initial slope.

Pulse-chase labeling

Experiments were performed as described (11). Briefly, CFBE cells expressing ΔF508-CFTR were pretreated with 3 μM VX-809 for 24 hours followed by 1-hour exposure to 1 or 0.1 μM VX-770. CFBE cells expressing ΔF508-CFTR-3S were exposed to 1 μM VX-770 for 1 hour. CFTR variants were pulse-labeled with [^{35}S]methionine and [^{35}S]cysteine (0.2 mCi/ml) (EasyTag EXPRESS Protein Labeling Mix, PerkinElmer) in cysteine- and methionine-free medium for 30 min and chased in full medium for 2.5 or 4.5 hours at 37°C in the presence of the indicated compounds. Radioactivity incorporated into the core- and

complex-glycosylated CFTR was visualized by fluorography and quantified by phosphorimage analysis with a Typhoon imaging platform (GE Healthcare).

Fluorescence ratiometric image analysis

The methodology for FRIA of endocytic vesicles containing CFTR as a cargo has been described in detail (43). Briefly, filter-grown CFBEi-ΔF508-3HA was allowed to polarize for 5 days and temperature-rescued for 48 hours at 30°C. VX-809 or VX-809 (3 μM) with 0.1 μM VX-770 was added for the last 24 hours and kept during the experiment. Before labeling, the cells were shifted to 37°C for 1.5 hours. Subsequently, rΔF508-CFTR-3HA was labeled with anti-HA antibody and FITC-conjugated goat anti-mouse secondary Fab (Jackson ImmunoResearch) on ice. Synchronized internalization was performed at the indicated times at 37°C. FRIA was performed on a Zeiss AxioObserver Z1 inverted fluorescence microscope (Carl Zeiss MicroImaging) equipped with an X-Cite 120Q fluorescence illumination system (Lumen Dynamics Group Inc.) and Evolve 512 EMCCD (electron-multiplying charge-coupled device) camera (Photometrics Technology). The acquisition was carried out at 495 ± 5–nm and 440 ± 10–nm excitation wavelengths with a 535 ± 25–nm emission filter and analyzed with MetaFluor software (Molecular Devices).

Planar lipid bilayer studies

Isolated CFTR-containing microsomes (containing 20 to 40 μg of total protein) were fused to planar lipid bilayers, and currents were analyzed as described previously (10, 11). Briefly, voltage was clamped at −60 mV, and currents were measured with a BC-535 amplifier (Warner Instrument) and pCLAMP 9 or 10 software (Axon Instruments), filtered at 200 Hz, and sampled at 10 kHz with an eight-pole Bessel filter and Digidata 1320 or 1440 digitizer (Axon Instruments). The chamber was gradually warmed from 23 to 37°C, reaching the maximum temperature within 8 to 9 min. Open probability (P_o) values were calculated for 2°C temperature intervals between 23 and 37°C, and the midpoints are depicted on the *x* axis.

Statistical analysis

Results are presented as means ± SEM, with the number of experiments indicated. Statistical analysis was performed by two-tailed Student's *t* test with the means of at least three independent experiments. The 95% confidence level was considered significant. For I_{sc} measurements, we performed paired *t* test analysis of patient/donor cells measured under different conditions. We used the Hill equation to calculate IC_{50} values in the GraphPad Prism software package. Original data and exact *P* values are provided in table S3.

Supplementary Material

Refer to Web version on PubMed Central for supplementary material.

Acknowledgments

We thank D. Gruenert (UCSF) for the parental CFBE41o− cell line, P. Wolters (UCSF) for assistance in collecting lung transplant tissues, R. J. Bridges (Rosalind Franklin University of Medicine and Science) and CFFT Inc. for CFTR modulator panels, P. J. Thomas (University of Texas Southwestern Medical Center Dallas, TX, USA) for the

pBI-CMV2-CFTR-P67L and -R347H plasmids, and V. Malhotra (Center for Genomic Regulation, Barcelona, Spain) for the HRP-C complementary DNA.

Funding: This work was supported by NIH DK72517 as well as the Research Development Program from the Cystic Fibrosis Foundation (to W.E.F. and A.S.V.), KTIA-AIK-12-2012-0025 (to T.H.), NIH–The National Institute of Diabetes and Digestive and Kidney Diseases R01DK75302, and Cystic Fibrosis Canada and Canadian Institutes of Health Research to (G.L.L). G.V. was partly supported by Fonds de Recherche Santé Québec Fellowship, and R.G.A. partly by the Solvay Fellowship and R.I. Birks Award. T.H. is a Bolyai Fellow of the Hungarian Academy of Sciences. G.L.L. is a Canada Research Chair.

REFERENCES AND NOTES

1. Collins FS. Cystic fibrosis: Molecular biology and therapeutic implications. Science. 1992; 256:774–779. [PubMed: 1375392]
2. Riordan JR. CFTR function and prospects for therapy. Annu. Rev. Biochem. 2008; 77:701–726. [PubMed: 18304008]
3. Rogan MP, Stoltz DA, Hornick DB. Cystic fibrosis transmembrane conductance regulator intracellular processing, trafficking, and opportunities for mutation-specific treatment. Chest. 2011; 139:1480–1490. [PubMed: 21652558]
4. Welsh MJ, Smith AE. Molecular mechanisms of CFTR chloride channel dysfunction in cystic fibrosis. Cell. 1993; 73:1251–1254. [PubMed: 7686820]
5. Du K, Sharma M, Lukacs GL. The ΔF508 cystic fibrosis mutation impairs domain-domain interactions and arrests post-translational folding of CFTR. Nat. Struct. Mol. Biol. 2005; 12:17–25. [PubMed: 15619635]
6. Okiyoneda T, Barrière H, Bagdány M, Rabeh WM, Du K, Höhfeld J, Young JC, Lukacs GL. Peripheral protein quality control removes unfolded CFTR from the plasma membrane. Science. 2010; 329:805–810. [PubMed: 20595578]
7. Rowe SM, Miller S, Sorscher EJ. Cystic fibrosis. N. Engl. J. Med. 2005; 352:1992–2001. [PubMed: 15888700]
8. Serohijos AW, Hegedus T, Aleksandrov AA, He L, Cui L, Dokholyan NV, Riordan JR. Phenylalanine-508 mediates a cytoplasmic–membrane domain contact in the CFTR 3D structure crucial to assembly and channel function. Proc. Natl. Acad. Sci. U.S.A. 2008; 105:3256–3261. [PubMed: 18305154]
9. Mendoza JL, Schmidt A, Li Q, Nuvaga E, Barrett T, Bridges RJ, Feranchak AP, Brautigam CA, Thomas PJ. Requirements for efficient correction of ΔF508 CFTR revealed by analyses of evolved sequences. Cell. 2012; 148:164–174. [PubMed: 22265409]
10. Okiyoneda T, Veit G, Dekkers JF, Bagdany M, Soya N, Xu H, Roldan A, Verkman AS, Kurth M, Simon A, Hegedus T, Beekman JM, Lukacs GL. Mechanism-based corrector combination restores ΔF508-CFTR folding and function. Nat. Chem. Biol. 2013; 9:444–454. [PubMed: 23666117]
11. Rabeh WM, Bossard F, Xu H, Okiyoneda T, Bagdany M, Mulvihill CM, Du K, di Bernardo S, Liu Y, Konermann L, Roldan A, Lukacs GL. Correction of both NBD1 energetics and domain interface is required to restore ΔF508 CFTR folding and function. Cell. 2012; 148:150–163. [PubMed: 22265408]
12. Ren HY, Grove DE, De La Rosa O, Houck SA, Sopha P, Van Goor F, Hoffman BJ, Cyr DM. VX-809 corrects folding defects in cystic fibrosis transmembrane conductance regulator protein through action on membrane-spanning domain 1. Mol. Biol. Cell. 2013; 24:3016–3024. [PubMed: 23924900]
13. Phuan PW, Veit G, Tan J, Roldan A, Finkbeiner WE, Lukacs GL, Verkman AS. Synergy-based small-molecule screen using a human lung epithelial cell line yields ΔF508-CFTR correctors that augment VX-809 maximal efficacy. Mol. Pharmacol. 2014; 86:42–51. [PubMed: 24737137]
14. Amin R, Ratjen F. Emerging drugs for cystic fibrosis. Expert Opin. Emerg. Drugs. 2014; 19:143–155. [PubMed: 24479826]
15. Galietta LJ. Managing the underlying cause of cystic fibrosis: A future role for potentiators and correctors. Paediatr. Drugs. 2013; 15:393–402. [PubMed: 23757197]

16. Rowe SM, Verkman AS. Cystic fibrosis transmembrane regulator correctors and potentiators. Cold Spring Harb. Perspect. Med. 2013; 3:a009761. [PubMed: 23818513]
17. Davis PB, Yasothan U, Kirkpatrick P. Ivacaftor. Nat. Rev. Drug Discov. 2012; 11:349–350. [PubMed: 22543461]
18. U.S. Food and Drug Administration approves KALYDECO™ (ivacaftor) for use in eight additional mutations that cause cystic fibrosis. 2014 Feb 21. press release http://investors.vrtx.com/releasedetail.cfm?ReleaseID=827435
19. Yu H, Burton B, Huang CJ, Worley J, Cao D, Johnson JP Jr, Urrutia A, Joubran J, Seepersaud S, Sussky K, Hoffman BJ, Van Goor F. Ivacaftor potentiation of multiple CFTR channels with gating mutations. J. Cyst. Fibros. 2012; 11:237–245. [PubMed: 22293084]
20. Results from phase 3 study of ivacaftor monotherapy showed statistically significant improvements in lung function in people with non-G551D gating mutations. 2013 Jul 29. press release http://investors.vrtx.com/releasedetail.cfm?ReleaseID=781005
21. Accurso FJ, Rowe SM, Clancy JP, Boyle MP, Dunitz JM, Durie PR, Sagel SD, Hornick DB, Konstan MW, Donaldson SH, Moss RB, Pilewski JM, Rubenstein RC, Uluer AZ, Aitken ML, Freedman SD, Rose LM, Mayer-Hamblett N, Dong Q, Zha J, Stone AJ, Olson ER, Ordoñez CL, Campbell PW, Ashlock MA, Ramsey BW. Effect of VX-770 in persons with cystic fibrosis and the G551D-CFTR mutation. N. Engl. J. Med. 2010; 363:1991–2003. [PubMed: 21083385]
22. Ramsey BW, Davies J, McElvaney NG, Tullis E, Bell SC, Dřevínek P, Griese M, McKone EF, Wainwright CE, Konstan MW, Moss R, Ratjen F, Sermet-Gaudelus I, Rowe SM, Dong Q, Rodriguez S, Yen K, Ordoñez C, Elborn JS. A CFTR potentiator in patients with cystic fibrosis and the *G551D* mutation. N. Engl. J. Med. 2011; 365:1663–1672. [PubMed: 22047557]
23. Bronsveld I, Mekus F, Bijman J, Ballmann M, de Jonge HR, Laabs U, Halley DJ, Ellemunter H, Mastella G, Thomas S, Veeze HJ, Tümmler B. Chloride conductance and genetic background modulate the cystic fibrosis phenotype of ΔF508 homozygous twins and siblings. J. Clin. Invest. 2001; 108:1705–1715. [PubMed: 11733566]
24. Van Goor F, Hadida S, Grootenhuis PD, Burton B, Cao D, Neuberger T, Turnbull A, Singh A, Joubran J, Hazlewood A, Zhou J, McCartney J, Arumugam V, Decker C, Yang J, Young C, Olson ER, Wine JJ, Frizzell RA, Ashlock M, Negulescu P. Rescue of CF airway epithelial cell function in vitro by a CFTR potentiator, VX-770. Proc. Natl. Acad. Sci. U.S.A. 2009; 106:18825–18830. [PubMed: 19846789]
25. Veeze HJ, Halley DJ, Bijman J, de Jongste JC, de Jonge HR, Sinaasappel M. Determinants of mild clinical symptoms in cystic fibrosis patients. Residual chloride secretion measured in rectal biopsies in relation to the genotype. J. Clin. Invest. 1994; 93:461–466. [PubMed: 8113384]
26. Kälin N, Claass A, Sommer M, Puchelle E, Tümmler B. ΔF508 CFTR protein expression in tissues from patients with cystic fibrosis. J. Clin. Invest. 1999; 103:1379–1389. [PubMed: 10330420]
27. Flume PA, Liou TG, Borowitz DS, Li H, Yen K, Ordoñez CL, Geller DE. VX 08-770-104 Study Group, Ivacaftor in subjects with cystic fibrosis who are homozygous for the F508del-CFTR mutation. Chest. 2012; 142:718–724. [PubMed: 22383668]
28. Van Goor F, Hadida S, Grootenhuis PD, Burton B, Stack JH, Straley KS, Decker CJ, Miller M, McCartney J, Olson ER, Wine JJ, Frizzell RA, Ashlock M, Negulescu PA. Correction of the F508 del-CFTR protein processing defect in vitro by the investigational drug VX-809. Proc. Natl. Acad. Sci. U.S.A. 2011; 108:18843–18848. [PubMed: 21976485]
29. Clancy JP, Rowe SM, Accurso FJ, Aitken ML, Amin RS, Ashlock MA, Ballmann M, Boyle MP, Bronsveld I, Campbell PW, De Boeck K, Donaldson SH, Dorkin HL, Dunitz JM, Durie PR, Jain M, Leonard A, McCoy KS, Moss RB, Pilewski JM, Rosenbluth DB, Rubenstein RC, Schechter MS, Botfield M, Ordoñez CL, Spencer-Green GT, Vernillet L, Wisseh S, Yen K, Konstan MW. Results of a phase IIa study of VX-809, an investigational CFTR corrector compound, in subjects with cystic fibrosis homozygous for the *F508del-CFTR* mutation. Thorax. 2012; 67:12–18. [PubMed: 21825083]
30. Final data from phase 2 combination study of VX-809 and KALYDECO™ (ivacaftor) showed statistically significant improvements in lung function in people with cystic fibrosis who have two copies of the F508del mutation. 2012 Jun 28. press release http://investors.vrtx.com/releasedetail.cfm?ReleaseID=687394

31. Two 24-week phase 3 studies of lumacaftor in combination with ivacaftor met primary endpoint with statistically significant improvements in lung function (FEV1) in people with cystic fibrosis who have two copies of the F508del mutation. 2014 Jun 24. press release http://investors.vrtx.com/releasedetail.cfm?releaseid=856185
32. Ehrhardt C, Collnot EM, Baldes C, Becker U, Laue M, Kim KJ, Lehr CM. Towards an in vitro model of cystic fibrosis small airway epithelium: Characterisation of the human bronchial epithelial cell line CFBE41o- Cell Tissue Res. 2006; 323:405–415. [PubMed: 16249874]
33. Veit G, Bossard F, Goepp J, Verkman AS, Galietta LJ, Hanrahan JW, Lukacs GL. Proinflammatory cytokine secretion is suppressed by TMEM16A or CFTR channel activity in human cystic fibrosis bronchial epithelia. Mol. Biol. Cell. 2012; 23:4188–4202. [PubMed: 22973054]
34. Pedemonte N, Lukacs GL, Du K, Caci E, Zegarra-Moran O, Galietta LJ, Verkman AS. Small-molecule correctors of defective ΔF508-CFTR cellular processing identified by high-throughput screening. J. Clin. Invest. 2005; 115:2564–2571. [PubMed: 16127463]
35. Access data FDA: 203188Orig1s000. http://www.accessdata.fda.gov/drugsatfda_docs/nda/2012/203188Orig1s000OtherRedt.pdf.
36. Snyder DS, Tradtrantip L, Yao C, Kurth MJ, Verkman AS. Potent, metabolically stable benzopyrimido-pyrrolo-oxazine-dione (BPO) CFTR inhibitors for polycystic kidney disease. J. Med. Chem. 2011; 54:5468–5477. [PubMed: 21707078]
37. Loo TW, Bartlett MC, Clarke DM. Corrector VX-809 stabilizes the first transmembrane domain of CFTR. Biochem. Pharmacol. 2013; 86:612–619. [PubMed: 23835419]
38. Neuberger T, Burton B, Clark H, Van Goor F. Use of primary cultures of human bronchial epithelial cells isolated from cystic fibrosis patients for the pre-clinical testing of CFTR modulators. Methods Mol. Biol. 2011; 741:39–54. [PubMed: 21594777]
39. Fulcher ML, Gabriel S, Burns KA, Yankaskas JR, Randell SH. Well-differentiated human airway epithelial cell cultures. Methods Mol. Med. 2005; 107:183–206. [PubMed: 15492373]
40. Lansdell KA, Cai Z, Kidd JF, Sheppard DN. Two mechanisms of genistein inhibition of cystic fibrosis transmembrane conductance regulator Cl− channels expressed in murine cell line. J. Physiol. 2000; 524(Pt. 2):317–330. [PubMed: 10766914]
41. Wang F, Zeltwanger S, Yang IC, Nairn AC, Hwang TC. Actions of genistein on cystic fibrosis transmembrane conductance regulator channel gating. Evidence for two binding sites with opposite effects. J. Gen. Physiol. 1998; 111:477–490. [PubMed: 9482713]
42. Apaja PM, Xu H, Lukacs GL. Quality control for unfolded proteins at the plasma membrane. J. Cell Biol. 2010; 191:553–570. [PubMed: 20974815]
43. Barrière H, Apaja P, Okiyoneda T, Lukacs GL. Endocytic sorting of CFTR variants monitored by single-cell fluorescence ratiometric image analysis (FRIA) in living cells. Methods Mol. Biol. 2011; 741:301–317. [PubMed: 21594793]
44. Hegedus T, Aleksandrov A, Cui L, Gentzsch M, Chang XB, Riordan JR. F508del CFTR with two altered RXR motifs escapes from ER quality control but its channel activity is thermally sensitive. Biochim. Biophys. Acta. 2006; 1758:565–572. [PubMed: 16624253]
45. Hoelen H, Kleizen B, Schmidt A, Richardson J, Charitou P, Thomas PJ, Braakman I. The primary folding defect and rescue of ΔF508 CFTR emerge during translation of the mutant domain. PLOS One. 2010; 5:e15458. [PubMed: 21152102]
46. Lewis HA, Zhao X, Wang C, Sauder JM, Rooney I, Noland BW, Lorimer D, Kearins MC, Conners K, Condon B, Maloney PC, Guggino WB, Hunt JF, Emtage S. Impact of the ΔF508 mutation in first nucleotide-binding domain of human cystic fibrosis transmembrane conductance regulator on domain folding and structure. J. Biol. Chem. 2005; 280:1346–1353. [PubMed: 15528182]
47. Protasevich I, Yang Z, Wang C, Atwell S, Zhao X, Emtage S, Wetmore D, Hunt JF, Brouillette CG. Thermal unfolding studies show the disease causing F508del mutation in CFTR thermodynamically destabilizes nucleotide-binding domain 1. Protein Sci. 2010; 19:1917–1931. [PubMed: 20687133]
48. Thibodeau PH, Richardson JM III, Wang W, Millen L, Watson J, Mendoza JL, Du K, Fischman S, Senderowitz H, Lukacs GL, Kirk K, Thomas PJ. The cystic fibrosis-causing mutation ΔF508

affects multiple steps in cystic fibrosis transmembrane conductance regulator biogenesis. J. Biol. Chem. 2010; 285:35825–35835. [PubMed: 20667826]

49. Haardt M, Benharouga M, Lechardeur D, Kartner N, Lukacs GL. C-terminal truncations destabilize the cystic fibrosis transmembrane conductance regulator without impairing its biogenesis. A novel class of mutation. J. Biol. Chem. 1999; 274:21873–21877. [PubMed: 10419506]
50. DeCarvalho AC, Gansheroff LJ, Teem JL. Mutations in the nucleotide binding domain-1 signature motif region rescue processing and functional defects of cystic fibrosis transmembrane conductance regulator ΔF508. J. Biol. Chem. 2002; 277:35896–35905. [PubMed: 12110684]
51. Farinha CM, King-Underwood J, Sousa M, Correia AR, Henriques BJ, Roxo-Rosa M, Da Paula AC, Williams J, Hirst S, Gomes CM, Amaral MD. Revertants, low temperature, and correctors reveal the mechanism of F508del-CFTR rescue by VX-809 and suggest multiple agents for full correction. Chem. Biol. 2013; 20:943–955. [PubMed: 23890012]
52. Bompadre SG, Cho JH, Wang X, Zou X, Sohma Y, Li M, Hwang TC. CFTR gating II: Effects of nucleotide binding on the stability of open states. J. Gen. Physiol. 2005; 125:377–394. [PubMed: 15767296]
53. Cui L, Aleksandrov L, Hou YX, Gentzsch M, Chen JH, Riordan JR, Aleksandrov AA. The role of cystic fibrosis transmembrane conductance regulator phenylalanine 508 side chain in ion channel gating. J. Physiol. 2006; 572:347–358. [PubMed: 16484308]
54. Xu Z, Pissarra LS, Farinha CM, Liu J, Cai Z, Thibodeau PH, Amaral MD, Sheppard DN. Revertant mutants modify, but do not rescue, the gating defect of the cystic fibrosis mutant G551D-CFTR. J. Physiol. 2014; 592:1931–1947. [PubMed: 24591578]
55. Van Goor F, Yu H, Burton B, Hoffman BJ. Effect of ivacaftor on CFTR forms with missense mutations associated with defects in protein processing or function. J. Cyst. Fibros. 2014; 13:29–36. [PubMed: 23891399]
56. Cholon DM, Quinney NL, Fulcher ML, Esther CR, Das J, Dokholyan NV, Randell SH, Boucher RC, Gentzsch M. Potentiator ivacaftor abrogates pharmacological correction of ΔF508 CFTR in cystic fibrosis. Sci. Transl. Med. 2014; 6:246ra96.
57. Guillot L, Beucher J, Tabary O, Le Rouzic P, Clement A, Corvol H. Lung disease modifier genes in cystic fibrosis. Int. J. Biochem. Cell Biol. 2014; 52:83–93. [PubMed: 24569122]
58. Xu W, Hui C, Yu SS, Jing C, Chan HC. MicroRNAs and cystic fibrosis—An epigenetic perspective. Cell Biol. Int. 2011; 35:463–466. [PubMed: 21476987]
59. European medicines agency, assessment report: Kalydeco EMA/473279/2012. http://www.ema.europa.eu/docs/en_GB/document_library/EPAR_-_Public_assessment_report/human/002494/WC500130766.pdf.
60. Wilschanski M, Dupuis A, Ellis L, Jarvi K, Zielenski J, Tullis E, Martin S, Corey M, Tsui LC, Durie P. Mutations in the cystic fibrosis transmembrane regulator gene and in vivo trans-epithelial potentials. Am. J. Respir. Crit. Care Med. 2006; 174:787–794. [PubMed: 16840743]
61. Suprynowicz FA, Upadhyay G, Krawczyk E, Kramer SC, Hebert JD, Liu X, Yuan H, Cheluvaraju C, Clapp PW, Boucher RC Jr, Kamonjoh CM, Randell SH, Schlegel R. Conditionally reprogrammed cells represent a stem-like state of adult epithelial cells. Proc. Natl. Acad. Sci. U.S.A. 2012; 109:20035–20040. [PubMed: 23169653]
62. Dekkers JF, Wiegerinck CL, de Jonge HR, Bronsveld I, Janssens HM, deWinter-de Groot KM, Brandsma AM, de Jong NW, Bijvelds MJ, Scholte BJ, Nieuwenhuis EE, van den Brink S, Clevers H, van der Ent CK, Middendorp S, Beekman JM. A functional CFTR assay using primary cystic fibrosis intestinal organoids. Nat. Med. 2013; 19:939–945. [PubMed: 23727931]
63. Yang H, Shelat AA, Guy RK, Gopinath VS, Ma T, Du K, Lukacs GL, Taddei A, Folli C, Pedemonte N, Galietta LJ, Verkman AS. Nanomolar affinity small molecule correctors of defective ΔF508-CFTR chloride channel gating. J. Biol. Chem. 2003; 278:35079–35085. [PubMed: 12832418]
64. Yamaya M, Finkbeiner WE, Chun SY, Widdicombe JH. Differentiated structure and function of cultures from human tracheal epithelium. Am. J. Physiol. 1992; 262:L713–L724. [PubMed: 1616056]

65. Namkung W, Finkbeiner WE, Verkman AS. CFTR-adenylyl cyclase I association responsible for UTP activation of CFTR in well-differentiated primary human bronchial cell cultures. Mol. Biol. Cell. 2010; 21:2639–2648. [PubMed: 20554763]

66. Namkung W, Thiagarajah JR, Phuan PW, Verkman AS. Inhibition of Ca^{2+}-activated Cl− channels by gallotannins as a possible molecular basis for health benefits of red wine and green tea. FASEB J. 2010; 24:4178–4186. [PubMed: 20581223]

67. Fiser A, Sali A. ModLoop: Automated modeling of loops in protein structures. Bioinformatics. 2003; 19:2500–2501. [PubMed: 14668246]

68. Pronk S, Páll S, Schulz R, Larsson P, Bjelkmar P, Apostolov R, Shirts MR, Smith JC, Kasson PM, van der Spoel D, Hess B, Lindahl E. GROMACS 4.5: A high-throughput and highly parallel open source molecular simulation toolkit. Bioinformatics. 2013; 29:845–854. [PubMed: 23407358]

69. MacKerell AD, Bashford D, Bellott M, Dunbrack RL, Evanseck JD, Field MJ, Fischer S, Gao J, Guo H, Ha S, Joseph-McCarthy D, Kuchnir L, Kuczera K, Lau FTK, Mattos C, Michnick S, Ngo T, Nguyen DT, Prodhom B, Reiher WE, Roux B, Schlenkrich M, Smith JC, Stote R, Straub J, Watanabe M, Wiórkiewicz-Kuczera J, Yin D, Karplus M. All-atom empirical potential for molecular modeling and dynamics studies of proteins. J. Phys. Chem. B. 1998; 102:3586–3616. [PubMed: 24889800]

70. Morris GM, Huey R, Lindstrom W, Sanner MF, Belew RK, Goodsell DS, Olson AJ. AutoDock4 and AutoDockTools4: Automated docking with selective receptor flexibility. J. Comput. Chem. 2009; 30:2785–2791. [PubMed: 19399780]

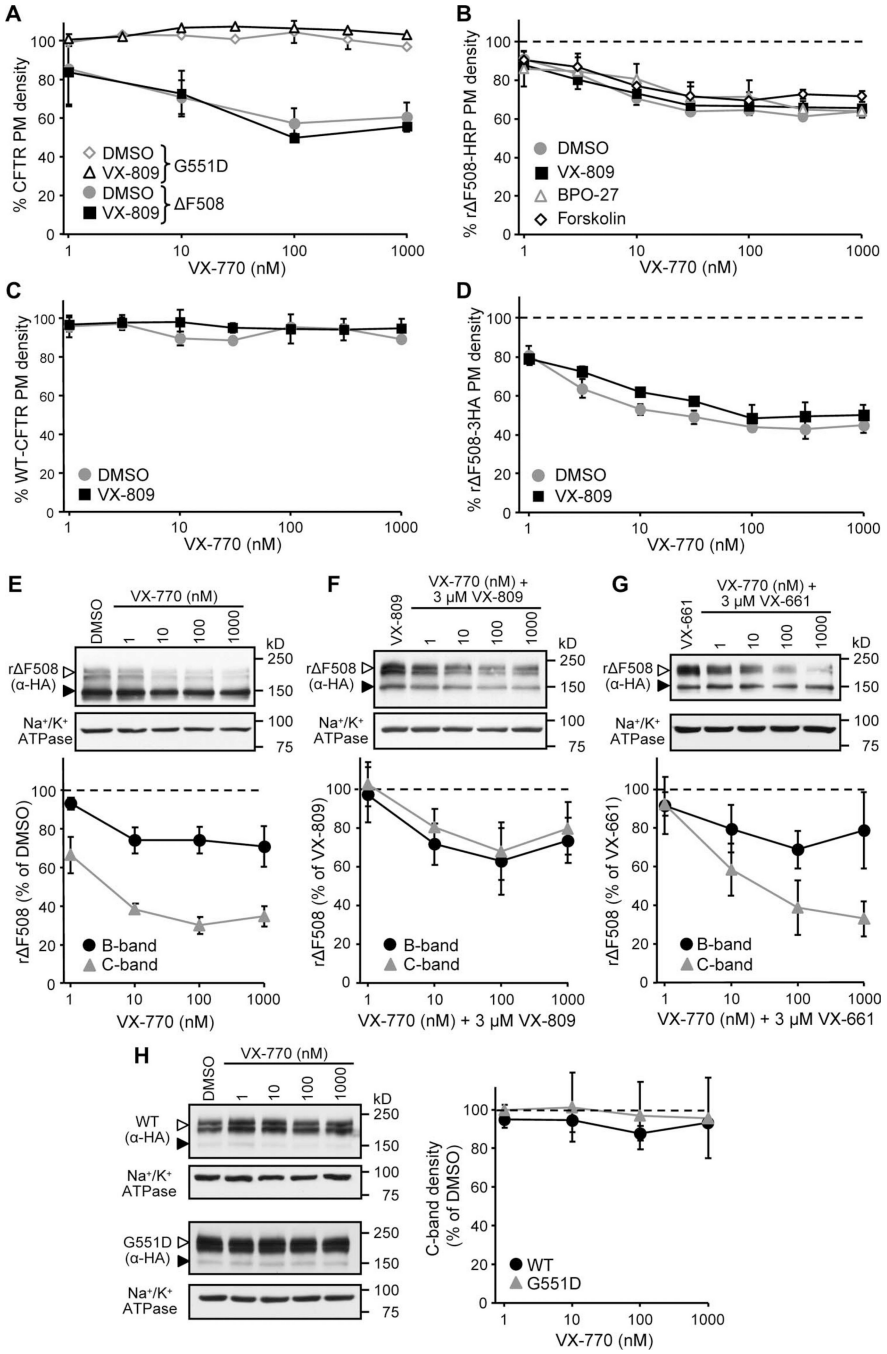

Fig. 1. Prolonged VX-770 exposure reduces the PM expression of ΔF508-CFTR but not wild-type (WT) or G551D-CFTR in human CFBE

(**A** and **C**) PM density of ΔF508-CFTR-HRP (ΔF508) (A), G551D-CFTR-3HA (G551D) (A), and WT-CFTR-3HA (C). Cells were treated with VX-770 for 24 hours in the presence or absence of 3 μM VX-809 at 37°C, and the values are expressed as percentage of non–VX-770-treated controls (n = 3). (**B** and **D**) PM density of low temperature (48 hours, 26°C)–rescued ΔF508-CFTR-HRP (rΔF508-HRP) (B) or ΔF508-CFTR-3HA (rΔF508-3HA) (D). Cells were treated with VX-770 in the presence or absence of VX-809 (3 μM), BPO-27

(25 μM), or forskolin (1 μM) for 24 hours at 26°C followed by a 1-hour chase at 37°C (n = 3). (**E** to **G**) Effect of VX-770 on the expression pattern of low temperature–rescued ΔF508-CFTR-3HA determined by immunoblot. Cells were treated with VX-770 alone (E) or in combination with VX-809 (3 μM) (F) or VX-661 (3 μM) (G) for 24 hours at 26°C. CFTR was visualized with anti-HA antibody, and anti–Na^+/K^+-ATPase antibody served as loading control. Densitometric analysis of the core-glycosylated (B-band, filled arrowhead) or complex-glycosylated (C-band, empty arrow-head) ΔF508-CFTR is expressed as percentage of control (lower panels, n = 3 to 4). (**H**) Effect of VX-770 on WT- and G551D-CFTR expression measured by immunoblot (left panel) and quantification of the C-band density (right panel, n = 3). Error bars indicate SEM of three or four independent experiments.

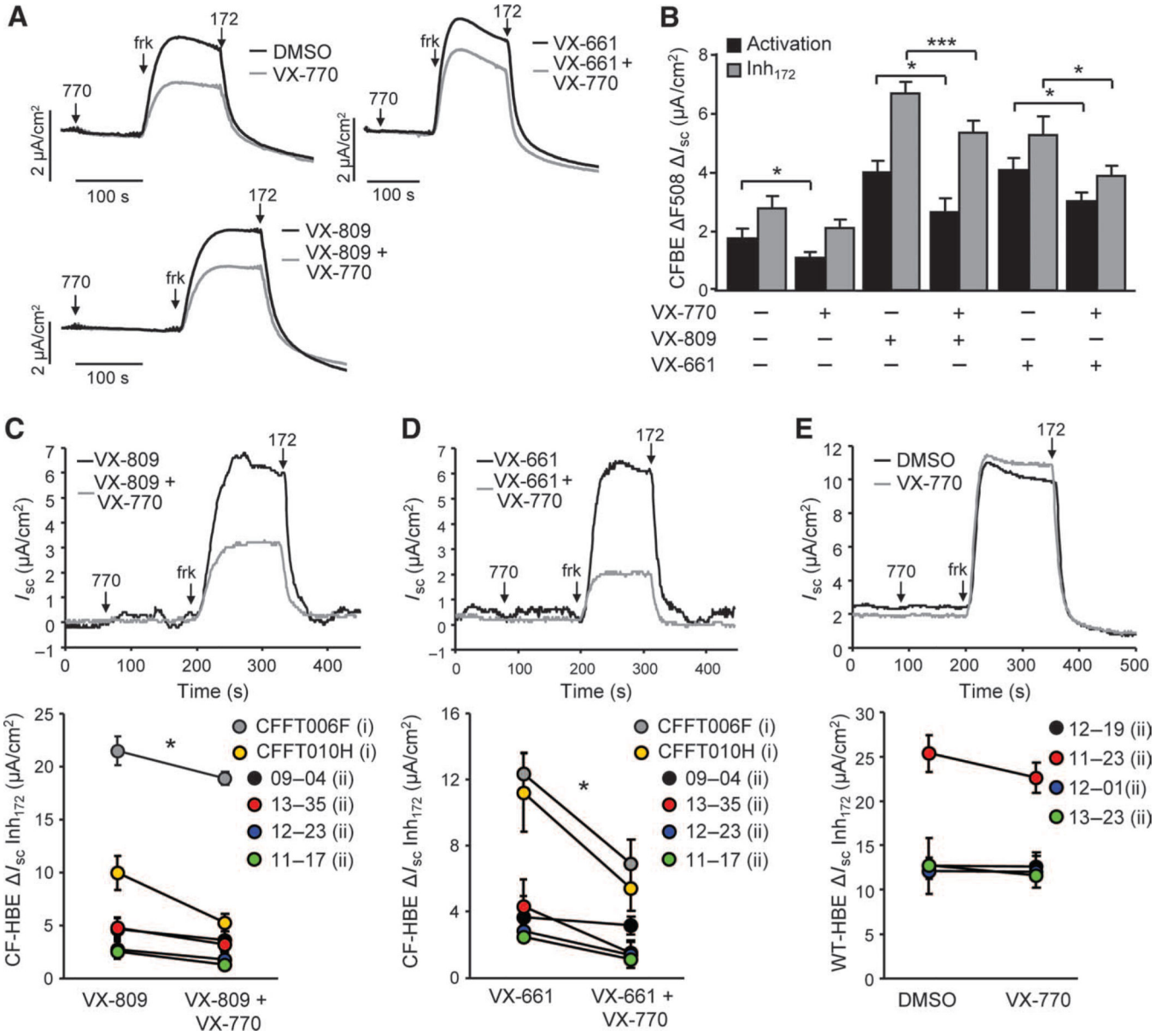

Fig. 2. Prolonged incubation with VX-770 reduces the maximal CFTR-mediated anion current in CFBE and primary cultures of ΔF508-CFTR but not WT-CFTR HBE

(**A** and **B**) Representative I_{sc} recordings (A) and quantification of the changes in I_{sc} (n = 3) (B) in CFBE monolayer expressing ΔF508-CFTR with or without 24-hour VX-770 (100 nM), VX-809 (3 μM), or VX-661 (3 μM) pretreatment. CFTR-mediated currents were induced by sequential acute addition of VX-770 (770, 10 μM) and forskolin (frk, 20 μM) followed by CFTR inhibition with Inh_{172} (172, 20 μM) in the presence of a basolateral-to-apical chloride gradient after basolateral permeabilization with amphotericin B. (**C** to **E**) Representative I_{sc} traces (upper panels) and quantification of the Inh_{172} inhibited current (ΔI_{sc} Inh_{172}, lower panels) in HBE isolated from six different homozygous ΔF508 CF patients (C and D) or four WT-CFTR donors (E) with or without VX-770 treatment (24 hours, 100 nM) alone (E) or in combination with VX-809 (3 μM) (C) and VX-661 (3 μM)

(D). The HBE cells were either polarized in Ultroser G medium (i) followed by measurement in the presence of a basolateral-to-apical chloride gradient and basolateral permeabilization with amphotericin B, or polarized in ALI medium (ii) and measured as an intact monolayer with equimolar chloride concentrations in both chambers. Error bars indicate SEM of three independent experiments (B) or SD of triplicate measurements (C to E). $*P < 0.05$, $***P < 0.001$ (exact P values are listed in table S3).

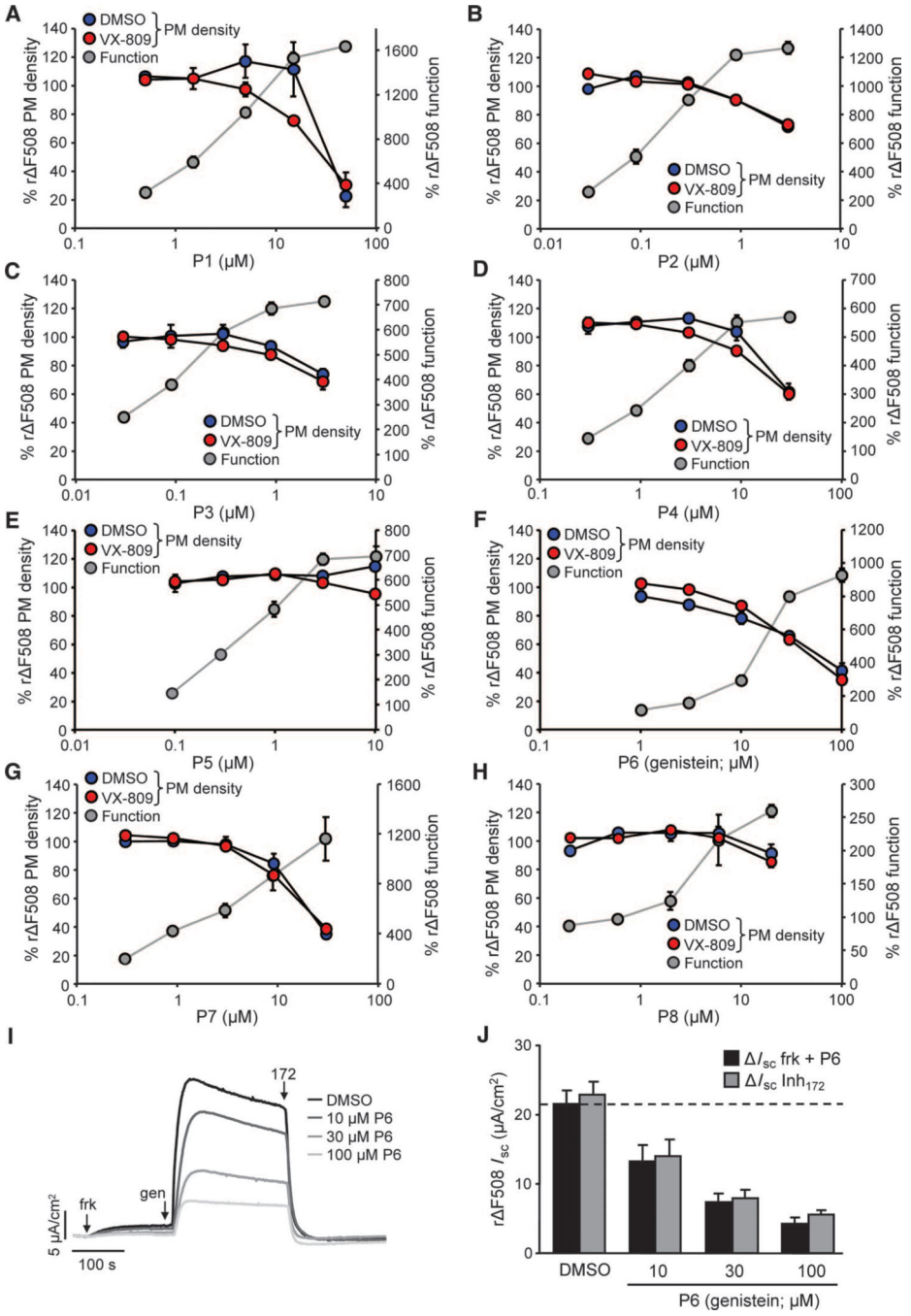

Fig. 3. Prolonged treatment with most potentiators reduces the PM density of rescued ΔF508-CFTR

(**A** to **H**) Effect of potentiators P1 (A), P2 (B), P3 (C), P4 (D), P5 (E), P6 (F), P7 (G), and P8 (H) on rΔF508-CFTR PM density in the presence or absence of 3 μM VX-809 (24-hour exposure, 26°C + 1-hour chase at 37°C, left axis, blue and red circles, $n = 3$) and function (acute addition, 32°C, right axis, gray circles, $n = 3$) in CFBE cells. (**I** and **J**) Representative I_{SC} recordings (I) and quantification of the changes in I_{SC} ($n = 3$) (J) in CFBE monolayer expressing rΔF508 with or without 24-hour P6 (genistein, 10 to 100 μM) pretreatment.

CFTR was activated by sequential acute addition of forskolin (20 μM) and genistein (10 to 100 μM) followed by CFTR inhibition with Inh_{172} (20 μM) in the presence of a basolateral-to-apical chloride gradient after basolateral permeabilization with amphotericin B. Error bars indicate SEM of three independent experiments.

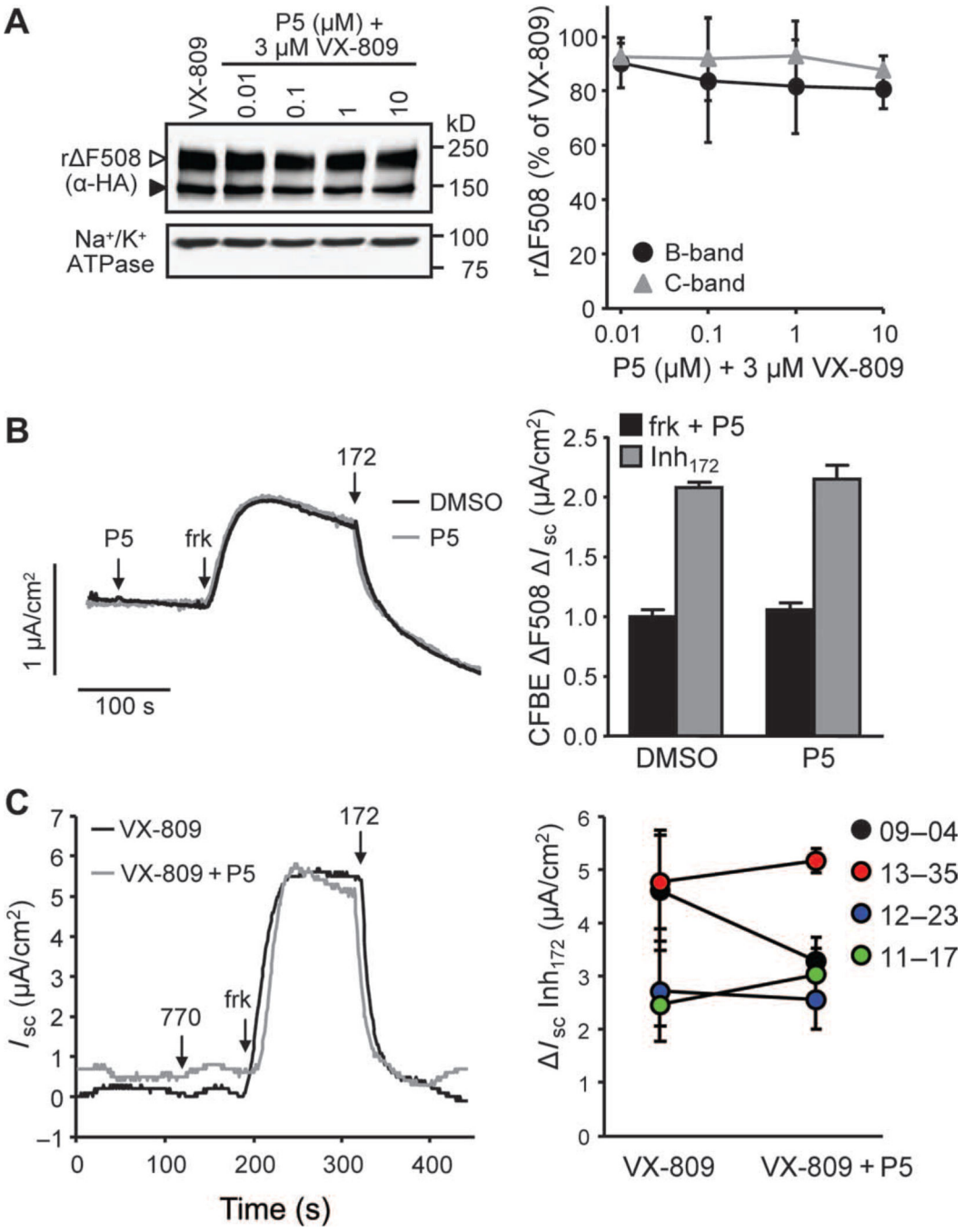

Fig. 4. Prolonged exposure to potentiator P5 does not impair the expression and function of ΔF508-CFTR

(**A**) Effect of P5 on the expression pattern of rΔF508, determined by immunoblot. Cells were treated with P5 in combination with VX-809, and CFTR was visualized using anti-HA antibody. Anti–Na^+/K^+-ATPase antibody served as loading control. Densitometric analysis of the core-glycosylated (B-band, filled arrowhead) or complex-glycosylated (C-band, empty arrowhead) rΔF508 is expressed as percentage of non–P5-treated controls (right panel, $n = 3$). (**B**) Representative I_{sc} recordings (left panel) and quantification of the changes

in I_{sc} (n = 3, right panel) in CFBE monolayer expressing ΔF508-CFTR with or without 24-hour P5 (3 μM) pretreatment. Measurements were performed in the presence of a basolateral-to-apical chloride gradient after basolateral permeabilization. (**C**) Representative I_{sc} traces (left panel) and quantification of the Inh_{172} inhibited current (ΔI_{sc} Inh_{172}, right panel) in HBE isolated from four different homozygous ΔF508 CF patients with or without P5 treatment (3 μM, 24 hours, 37°C) in combination with VX-809 (3 μM). The HBE cells were polarized in ALI medium and measured without permeabilization with symmetrical chloride-containing solutions. Error bars indicate SEM of three independent experiments (A and B) or SD of triplicate measurements (C).

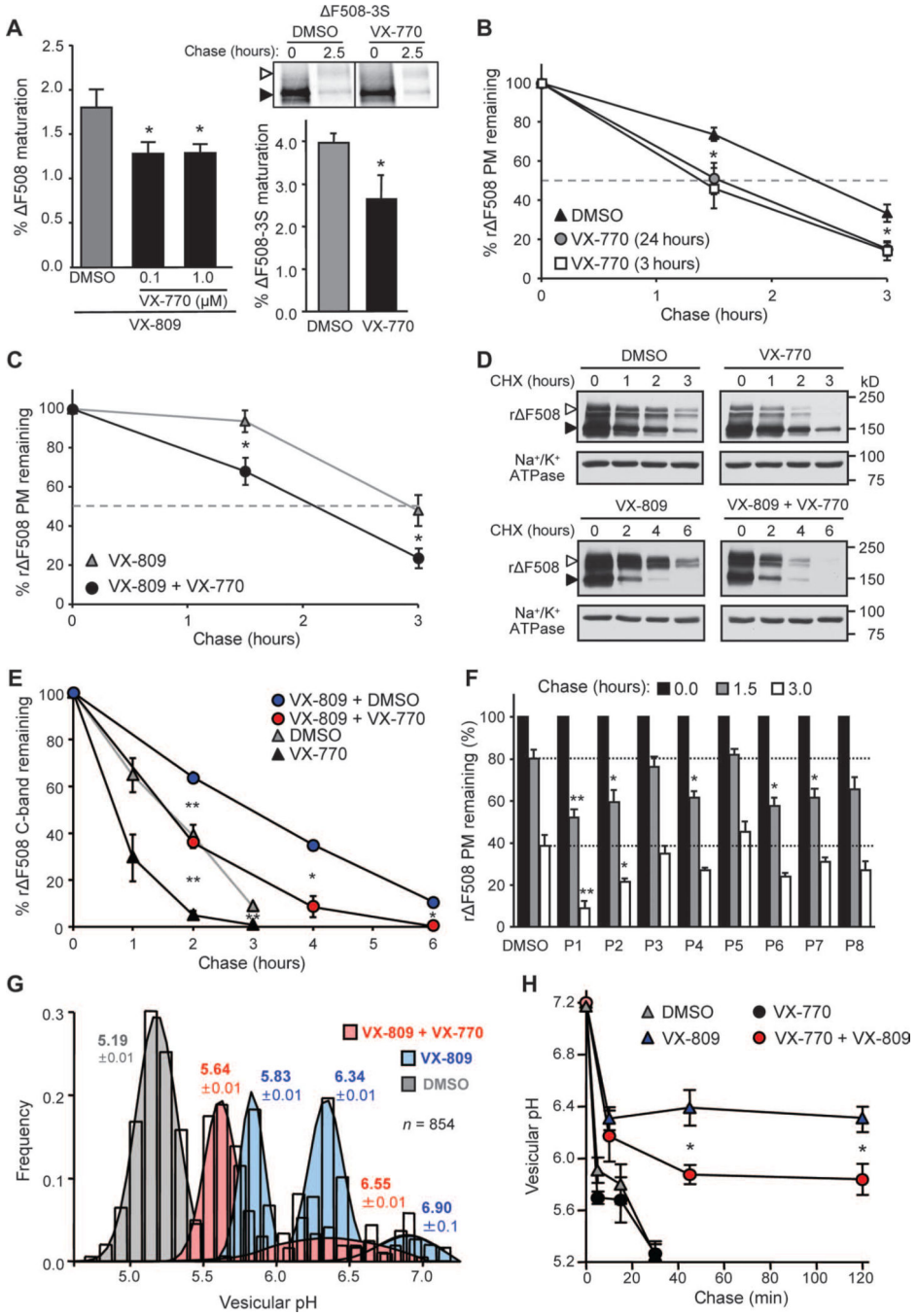

Fig. 5. VX-770 attenuates the maturation and accelerates the PM removal of ΔF508-CFTR

(**A**) Determination of ER folding efficiency of ΔF508-CFTR in the presence of VX-809 (3 μM, 24 hours, left panel, *n* = 5) or of ΔF508-3S in the absence of VX-809 (right panel, *n* = 3) by metabolic pulse-chase in CFBE cells with or without VX-770 (1.0 or 0.1 μM, 1-hour pretreatment). The folding efficiency was calculated as the percentage of pulse-labeled, immature core-glycosylated ΔF508-CFTR (B-band, filled arrowhead) conversion into the mature complex-glycosylated form (C-band, open arrowhead). Labeling was performed for 30 min followed by chase for 2.5 hours at 37°C. (**B** and **C**) Effect of VX-770 on the PM

stability of low temperature– rescued (48 hours, 26°C) ΔF508-CFTR (rΔF508). CFBE monolayer was treated with VX-770 (1 μM, 3 or 24 hours, 26°C) alone (B) or in combination with VX-809 (3 μM) (C) followed by chase at 37°C for 1.5 or 3 hours ($n = 4$). (**D**) Stability of rΔF508 in CFBE cells treated with VX-770 (100 nM, 24 hours) and VX-809 (3 μM, 24 hours) was determined by immunoblot with CHX chase. (**E**) Complex-glycosylated CFTR [open arrowhead in (D)] disappearance was quantified by densitometry and is expressed as percentage of initial amount ($n = 3$). (**F**) Effect of each potentiator (P1, P4, P7, and P8, 30 μM; P2 and P3, 3 μM; P5, 10 μM; and P6, 100 μM; 24 hours, 26°C) on the PM stability of rΔF508 ($n = 3$). (**G**) Representative histogram of rΔF508-containing vesicular pH measured by FRIA. The cells were treated with dimethyl sulfoxide (DMSO), VX-809 (3 μM), or VX-809 and 0.1 μM VX-770 for 24 hours and during the 120-min chase. The Gaussian distribution of the vesicular pH of 280 vesicles is indicated for each condition. (**H**) Influence of VX-770 on the endolysosomal transfer kinetics of rΔF508. The graph shows the mean vesicular pH at each chase point ($n = 3$). Error bars indicate SEM of three to five independent experiments. $^{*}P < 0.05$, $^{**}P < 0.01$ (exact P values are listed in table S3).

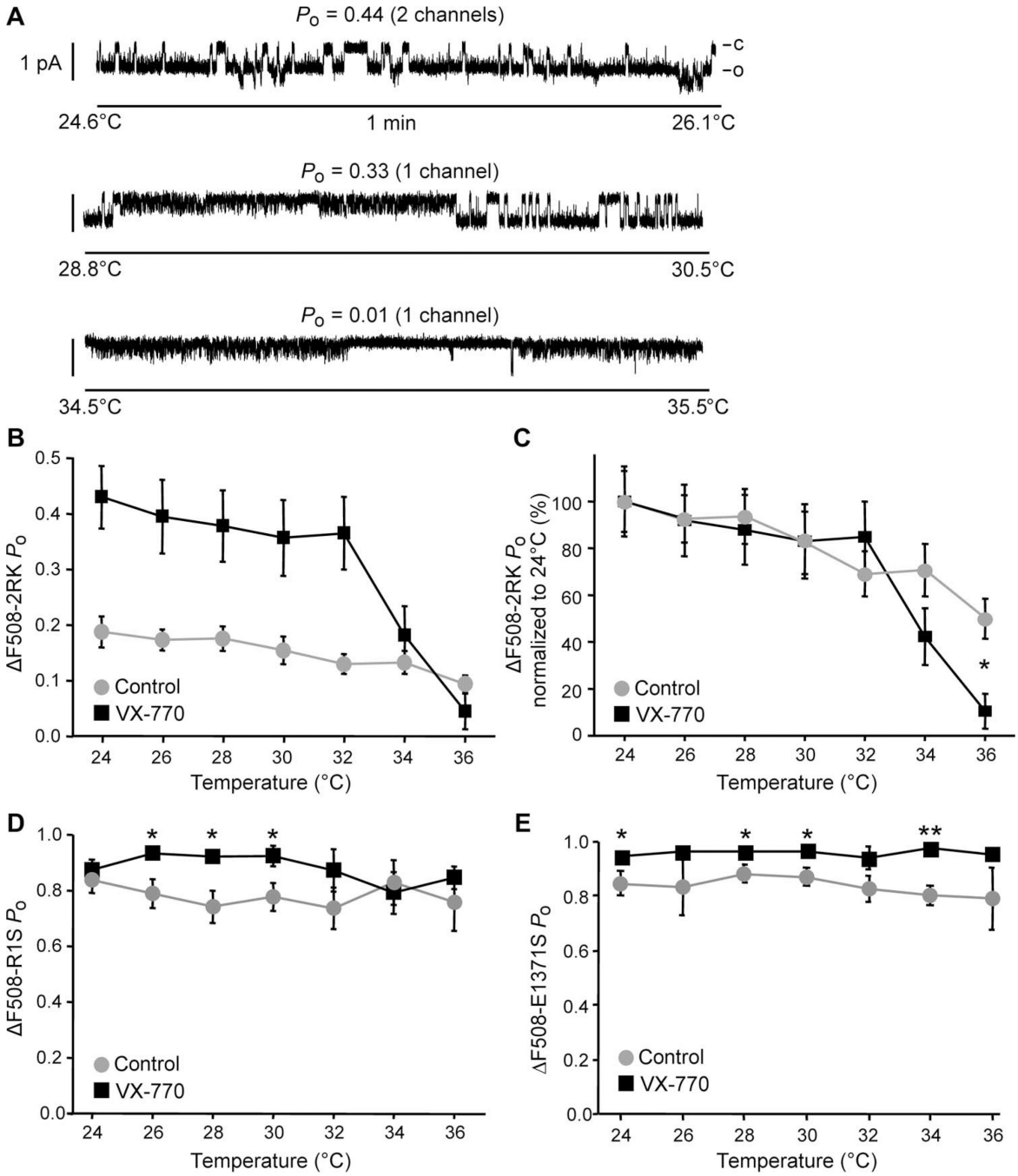

Fig. 6. VX-770 directly interacts with and destabilizes the ΔF508-CFTR-2RK channel

(**A**) Representative records show ΔF508-R29K-R555K-CFTR (ΔF-2RK) channel function in the presence of 1 μM VX-770 from two separate experiments at ~25°C (two channels incorporated), ~30°C, and ~35°C (one channel incorporated). The closed (c) and open (o) states of the channels are indicated. (**B**) Single-channel open probabilities (P_o) of protein kinase A–activated ΔF508-CFTR-2RK in the presence or absence of VX-770 (1 μM) (n = 7 to 46). The cumulative duration of single-channel measurements for any given temperature exceeded 8.5 min. (**C**) Temperature-dependent inactivation of ΔF508-2RK in the presence

or absence of VX-770 (1 μM) derived by normalization with 24°C values of the results depicted in (B). (**D** and **E**) Single-channel open probabilities (P_o) of protein kinase A–activated ΔF508-CFTR-R1S (ΔF508-R1S, n = 4 to 13) (D) or ΔF508-CFTR-E1371S (ΔF-E1371S, n = 4 to 6) (E) determined by artificial phospholipid bilayer measurements in the presence or absence of VX-770 [1 μM in (D), 0.1 μM in (E)]. The cumulative measurement time for any given temperature was >4.5 min for ΔF508-R1S and >3 min for ΔF508-E1371S. Error bars indicate SEM of 4 to 46 independent experiments. *P < 0.05, **P < 0.01 (exact P values are listed in table S3).

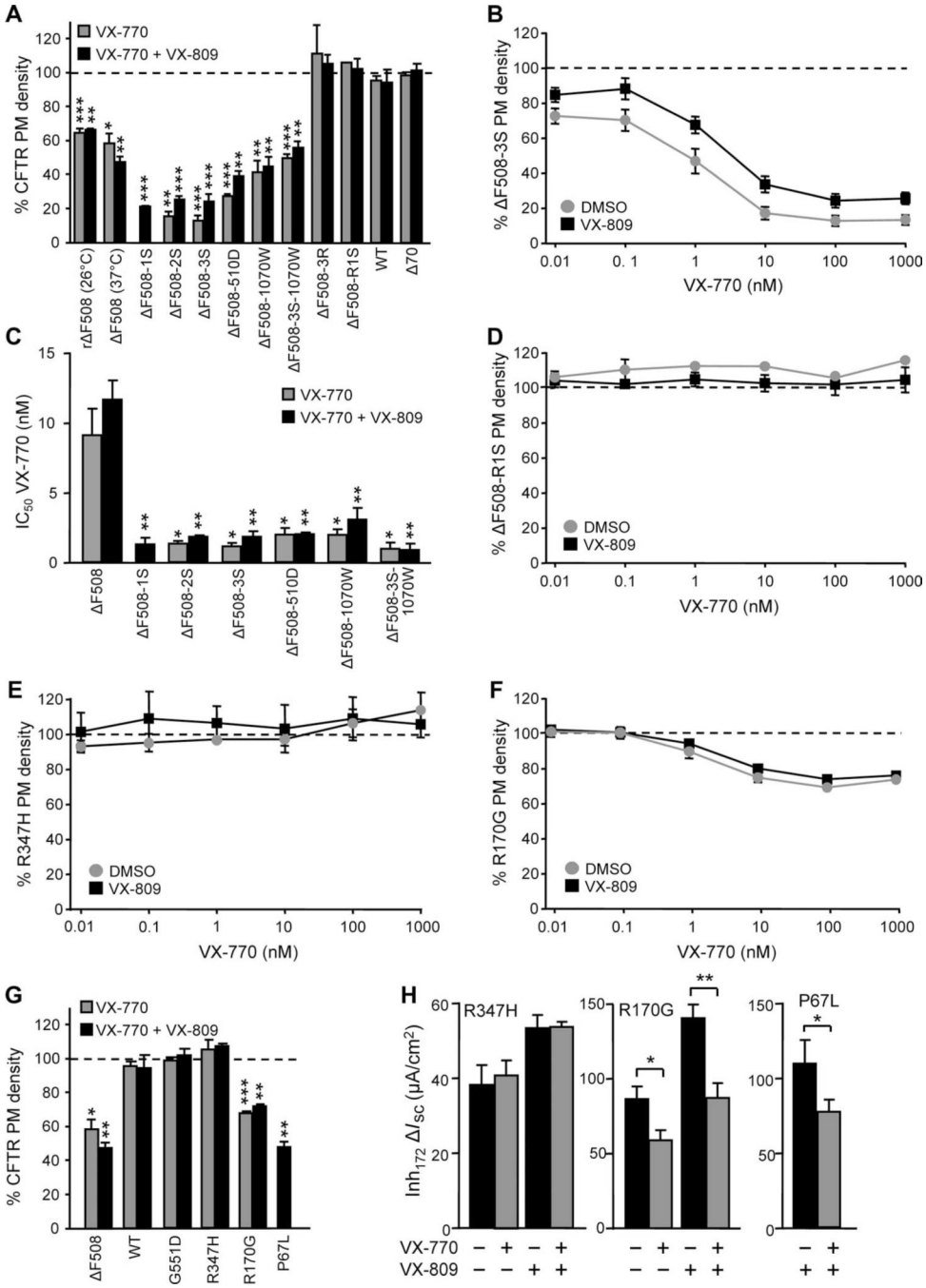

Fig. 7. Suppressor mutations of ΔF508-CFTR and other CF-causing CFTR mutations modulate the susceptibility to VX-770– mediated PM down-regulation

(**A**) PM density of ΔF508-CFTR with or without second-site suppressor mutations and of non–ΔF508-CFTR variants was measured after VX-770 (100 nM, 24 hours) incubation (n = 3). (**B** and **D**) PM density of ΔF508-3S (B) (n = 3) and ΔF508-R1S (D) (n = 3) after 24 hours of treatment with increasing concentrations of VX-770 in the presence or absence of VX-809 (3 μM). (**C**) 50% inhibitory concentration (IC_{50}) of VX-770 on CFTR variants' PM expression, calculated on the basis of the measurements shown in (B), (D), and fig. S5 (B to

F). (**E** and **F**) PM density of R347H-CFTR (E) and R170G-CFTR (F) after 24 hours of treatment with increasing concentrations of VX-770 in the presence of DMSO or VX-809 (3 μM). (**G**) CFTR PM density after VX-770 (100 nM, 24 hours) incubation, measured for CF-causing mutants G551D-, R347H-, R170G-, and P67L-CFTR ($n = 3$). The values for ΔF508- and WT-CFTR are shown for comparison. (**H**) Quantification of the changes in I_{sc} ($n = 3$) (B) in CFBE monolayers expressing R347H-, R170G-, or P67L-CFTR with or without 24-hour VX-770 (100 nM) and VX-809 (3 μM) pretreatment ($n = 3$ to 4). Error bars indicate SEM of three to four independent experiments. *$P < 0.05$, **$P < 0.01$, ***$P < 0.001$ (exact P values are listed in table S3).

Table 1

Effect of 24 hours of potentiator treatment on I_{sc} measurements of primary *CFTR*$^{\Delta F508/\Delta F508}$ HBE.

Patient	Differentiation medium	VX-809					VX-661		
		DMSO Mean ± SD (μA/cm^2)	VX-770 Mean ± SD (μA/cm^2)	Change %	P5 Mean ± SD (μA/cm^2)	Change %	DMSO Mean ± SD (μA/cm^2)	VX-770 Mean ± SD (μA/cm^2)	Change %
09-04	ALI (39)	4.61 ± 1.13	3.63 ± 1.17	−21	3.30 ± 0.44	−28	3.67 ± 1.27	3.17 ± 0.55	−14
13-35	ALI	4.77 ± 0.88	3.18 ± 0.17	−33	5.17 ± 0.23	8	4.33 ± 1.63	1.53 ± 0.74	−65
12-23	ALI	2.72 ± 0.94	1.78 ± 0.94	−35	2.57 ± 0.55	−6	2.85 ± 0.35	1.38 ± 0.79	−52
11-17	ALI	2.47 ± 0.40	2.47 ± 0.40	−49	3.03 ± 0.49	23	2.47 ± 0.15	1.13 ± 0.23	−54
Mean	ALI	3.64	2.46	−34	3.52	−1	3.33	1.80	−46
CFFT006F	Ultroser G (38)	21.52 ± 1.38	18.89 ± 0.59	−12	n.d.	n.d.	12.34 ± 1.27	6.90 ± 1.48	−44
CFFT010H	Ultroser G	9.95 ± 1.62	5.26 ± 0.80	−47	n.d.	n.d.	11.21 ± 2.36	5.44 ± 1.37	−51
Mean	Ultroser G	15.74	12.07	−30			11.78	6.17	−48
Combined (mean ± SEM)				−33 ± 6		−1 ± 11			−47 ± 8

n.d., not determined.